Effect of Moisture on Tensile Strength of Bulk Solids II: Fine Particle-Size Materials with Varying Inherent Coherence

TERENCE EAVES* and TREVOR M. JONES▲

Abstract □ The effect of moisture on the tensile strength of a variety of fine particle-size bulk solids at fixed states of packing is reported. The values of tensile strength obtained are examined quantitatively in terms of the components of force contributing to the overall strength. For inherently cohesive materials, equations relating the separation distance at the surface asperities of the individual particles to the effect of van der Waals' forces show good agreement with experimental results for dry powders. When the materials are moist, the mean equivalent separation distances are shown to be related to the average length of the macroscopic liquid bridges and not to the microcontact distances. For noncohesive materials, calculation of the tensile strength from equations relating to the liquid pendular bonds is satisfactory when the interparticle distance is estimated from the geometry of the packing. Calcium phosphate showed no change in tensile strength with increased moisture content up to about 50% w/w due to its porous internal nature.

Keyphrases □ Tensile strength, bulk solids—effect of moisture on fine particle-size materials with varying inherent coherence □ Moisture—effect on tensile strength of fine particle-size materials with varying inherent coherence □ Particle size of bulk solids, fine—effect of moisture on tensile strength

In a previous paper (1), the observed differences in the effects of moisture on the tensile strength of fine and coarse sodium chloride fractions were attributed to two possible causes: (*a*) the production of fewer pendular bonds at points of near contact by the finer fractions because of their lower porosities (*i.e.*, basically a particle-size effect), and (*b*) the progressive disruption, in the fine fractions, of the particle–particle interactions present at dryness (*i.e.*, an effect dependent on the coherence of the dry material).

In this paper, further work is reported on the effects of moisture on the tensile strength of bulk solids of similar particle size which, when dry, show differing degrees of coherence at similar porosities.

EXPERIMENTAL

Materials—Details of the calcium phosphate, glass, and potassium chloride used are shown in Table I and Fig. 1. The potassium chloride showed a tendency to cake on standing in the laboratory, a phenomenon found to be dependent on the degree of consolidation and the presence of moisture. Consequently, immediately after preparation it was stored in a lightly dredged state in layers 5 mm. thick in a hot air oven at 120°.

Since particle diameters determined using the Coulter counter are those of spheres of equivalent volume, one expects the calculated specific surfaces (Table I) to be lower than the measured values since none of the materials consists of regular spheres. However, the vast difference in values for calcium phosphate could not be accounted for simply by departure from sphericity, but it is indicative of the porous nature of the particles.

Procedure—Samples of each material were dried in loosely dredged layers less than 5 mm. thick in 10.16 × 6.35 × 1.27-cm. (4 × 2.5 × 0.5-in.) aluminum foil trays at 120° for 40 hr. They were then transferred hot to a specially constructed temperature and humidity controlled cabinet (2) previously equilibrated at 28° and a relative humidity below 25%. Tensile strength determinations were carried out as previously described (1) using consolidating stresses between 0 and 202 g. cm.$^{-2}$. Tensile tests were also performed after various periods of exposure to relative humidities up to 75% and after the addition of various percentages (by weight) of distilled water (to calcium phosphate and glass) or saturated (28°) potassium chloride solution (to potassium chloride). The moisture content of each sample was determined after testing by drying to a constant weight at 120°.

The surface tensions and viscosities of the distilled water and potassium chloride solution were determined by means of a tensiometer[1] fitted with a platinum ring and a viscometer[2] using measuring system 0.

RESULTS AND DISCUSSION

Previous studies (3) showed the necessity for calculating packing density on the basis of the weight of undissolved solid only. Of the materials studied, it is assumed that the calcium phosphate and glass are insoluble in water and that the concentration of the saturated potassium chloride solution at 28° is 37.0 g./100 g. water[3]. Thus, if W_u is the weight of undissolved solid in the test cell and W_w is the total weight of the moist material in the test cell, $W_u = W_w$ for calcium phosphate and glass, and $W_u = W_w[(100 - 0.37b)/(100 + b)]$ for potassium chloride, where b = percentage weight loss on drying, dry basis.

Figure 2 shows the effect of consolidation on tensile strength for the three bulk solids at the lowest moisture contents achieved. The corresponding curves for fine sodium chloride fractions, taken from Eaves and Jones (1), are also shown for comparison. It is clear that the coherence of the calcium phosphate, as denoted by the tensile strength at a fixed packing density (*i.e.*, fixed porosity) was greater than that of potassium chloride, which was greater than that of glass.

At higher moisture contents, similar plots of tensile strength *versus* packing density were obtained and double log regression lines (4) were fitted to the points by computer. From these lines, curves showing tensile strength changes with moisture content at fixed packing densities were constructed (Figs. 3–5), as for the sodium chloride fractions previously (1).

The glass (Fig. 3) showed an increase in tensile strength toward a plateau as the moisture content increased and, in this respect, resembled the coarse sodium chloride fractions (1), whereas the potassium chloride (Fig. 4) showed an initial increase to a maximum (similar to the fine sodium chloride fractions). The calcium phosphate, however (Fig. 5), was unusual in that there was little change in tensile strength even at 50% w/w moisture content (dry basis).

Consideration of Fig. 3 shows that at the higher packing densities the tensile strength of the glass continued to increase. This was probably due to the moisture becoming located in the funicular state, when the tensile strength becomes a function of the entry suction of the saturated (capillary) system (5). In practice, onset of the funicular state is marked by the fusion of adjacent liquid bridges (5) which will occur at lower moisture contents for higher packing densities.

With these different materials, the wetting fluid is not the same in each case (since potassium chloride and sodium chloride are water

[1] Du Nouy, Cambridge Instruments, Ltd., Cambridge, England.
[2] Epprecht Rheomat-15, Contraves, Ltd., Zürich, Switzerland.
[3] "Handbook of Chemistry and Physics," 1947.

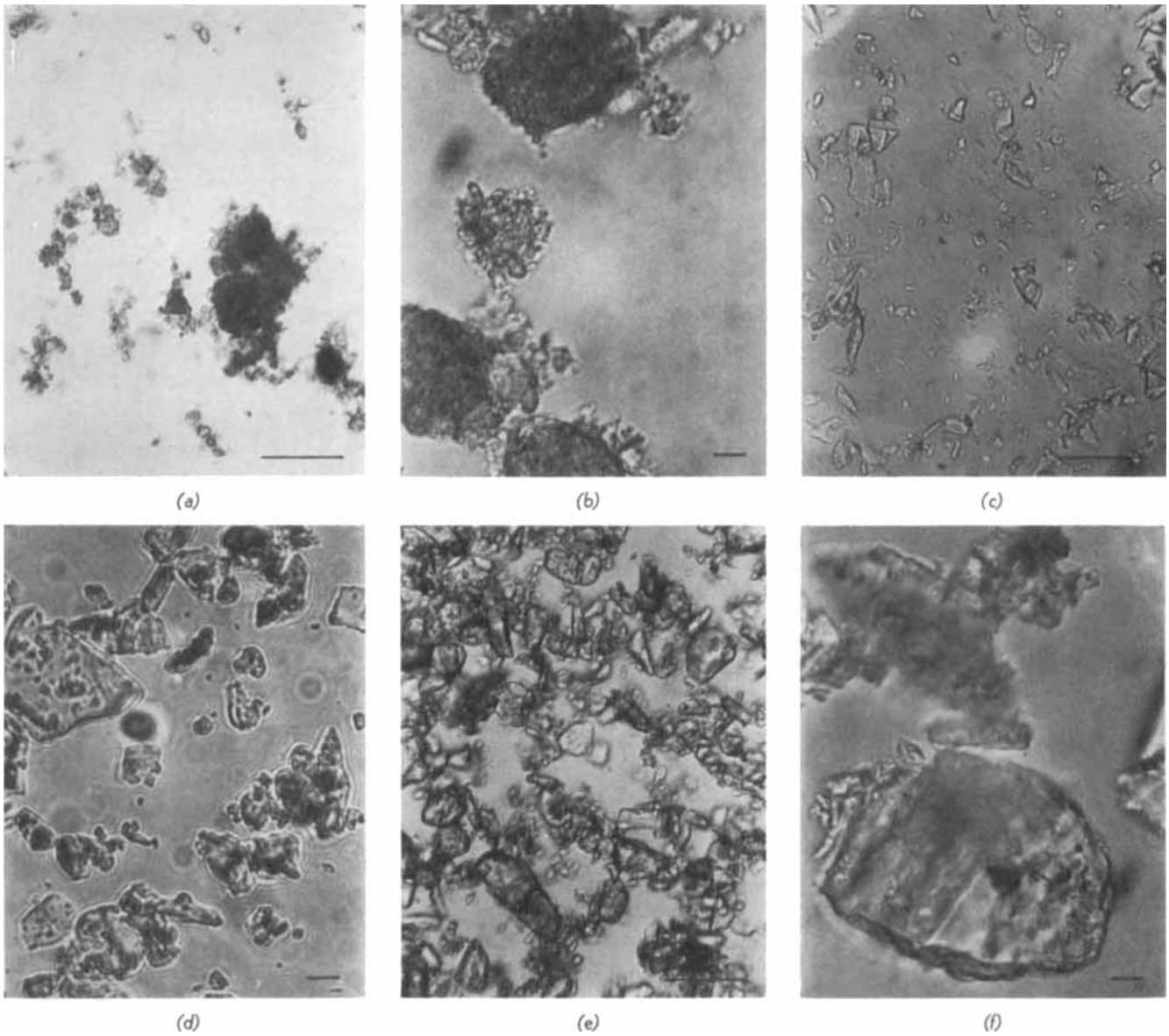

Figure 1—*Typical photomicrographs of the materials used. Key:* (a) *and* (b), *calcium phosphate;* (c) *and* (d), *glass; and* (e) *and* (f), *lactose. Scale marks:* (a), (c), *and* (e) = *100 μ; and* (b), (d), *and* (f) = *10 μ.*

soluble), so properties of the wetting fluid that might influence the tensile strength [*i.e.*, surface tension and possibly viscosity (6)] must be taken into account. However, the viscosities of the wetting fluids were almost identical (Table II). Furthermore, different effects were demonstrated when the surface tension was constant [between the coarse and fine fractions of sodium chloride (1)], and similar effects were demonstrated when the surface tension was different (between the glass and coarse sodium chloride fractions). It seems, therefore, that the different effects of moisture arise from the different nature of the materials.

Table I—Physical Characteristics of Bulk Solids Used

	Origin and Method of Preparation	Particle Density, g. cm.$^{-3}$	Particle Shape Description According to British Standard 2955(1958)	Elongation Ratio	Mass Median Coulter Diameter, μ	Specific Surface, m.^{2} g.$^{-1}$	
						Strohlein	Calculated from Coulter Data
Calcium phosphate	BPC grade, Boots Ltd.	2.96	Granular	1.51	9	23.2	0.33
Powdered glass	British Drug Houses Ltd.	2.54	Acicular and angular	1.85	18	0.71	0.19
Potassium chloride	BP grade, McCarthy's Ltd., End-runner milled and less than 32-μ fraction used	1.96	Irregular	1.32	15	0.74	0.31

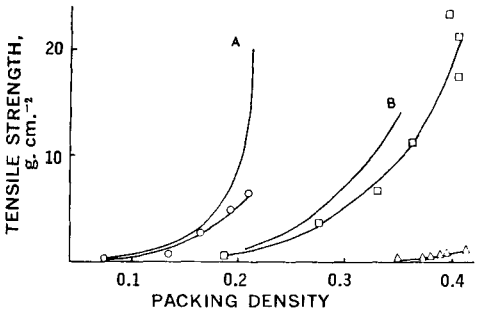

Figure 2—*Tensile strengths of dried materials at packing densities produced by consolidating stresses from 0 to 101.9 g. cm.$^{-2}$.*

	Mass Median Diameter, μ	*Average Moisture Content (% w/w), Dry Basis*
O, *Calcium phosphate*	*9*	*0.5*
□, *Potassium chloride*	*15*	*0.1*
△, *Glass*	*18*	*0.2*
A, Sodium chloride	*5*	*0.1*
B, Sodium chloride	*14*	*0.04*

The curves shown are taken from the double log regression lines.

Consider first the potassium chloride and glass. Since the particle sizes and distributions were similar, it follows from the two possible explanations stated at the beginning of this paper that the different effects of moisture on the tensile strength of beds of these materials at the same packing density were probably due to the differences in initial dry coherence. It is, therefore, suggested that the coherence arising from particle–particle interactions (probably van der Waals' or mechanical interactions) in a dry, cohesive material is, after a possible initial increase (due to immobile adsorbed layers), only reduced *little by little* as the moisture content increases. This may be due to a graded reduction in the magnitude of van der Waals' (or mechanical) forces in the presence of increasing amounts of mobile water. More probable, however, is the reduction of these forces to zero by the presence of mobile water, with the graded reduction in inherent coherence stemming from the persistence of fewer dry points of interaction at successively higher moisture contents. This would fit in well with the previous suggestion (1) that new pendular bonds are created at points of actual contact as the moisture content of a bulk solid increases. Therefore, of the possible mechanisms suggested to be responsible for the two types of tensile strength changes produced by moisture, the most likely are summarized in Fig. 6.

Aoki and Tsunakawa (7) also studied the effects of moisture on inherently cohesive materials. They found that flyash, calcium carbonate, white alundum, and alumina at fixed porosities showed increases (but no subsequent decreases) in tensile strength as the

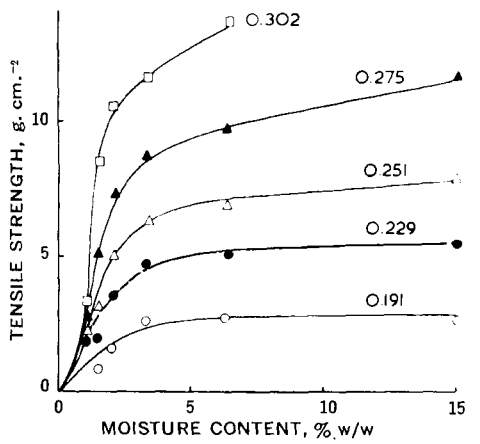

Figure 3—*Effect of moisture content (% w/w, dry basis) on tensile strength of glass at the packing densities shown.*

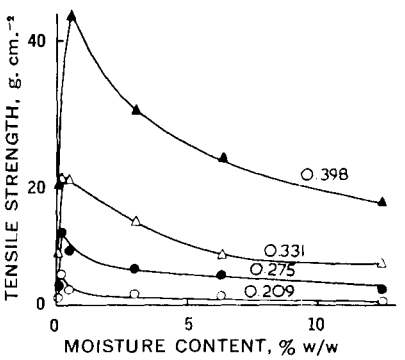

Figure 4—*Effect of moisture content (% w/w, dry basis) on tensile strength of potassium chloride at the packing densities shown.*

moisture content increased. Since they only considered moisture contents up to 3% (by volume), they may not have reached the stage with these materials at which the decrease occurred. Similarly, studies involving other flow parameters have used only low moisture contents over which progressive flow impairment (*i.e.*, presumably an increased tensile strength) occurred. For example, Craik and Miller (8) showed increases in the angle of repose of sodium chloride and sucrose (both approximately 10 μ) up to moisture contents of 0.14 and 0.20%, respectively.

The tensile strength of the calcium phosphate (Fig. 5) remained unchanged probably because the moisture was located initially within the porous particles (not at the surface) and did not affect the particle–particle interactions until the particles became saturated. This point could not be reached, since above 50% w/w moisture content (dry basis) the material became pastelike and impossible to test. It was likewise suggested by Glushkov *et al.* (9) that the internal friction of materials composed of porous particles increased only after saturation of this internal structure. However, the independence of the tensile strength of calcium phosphate on moisture content may also be due to a balance of those components of tensile strength already discussed and summarized (Fig. 6) for nonporous materials.

Having established the components of tensile stength of the various bulk solids investigated (Fig. 6), it is possible to examine their experimentally determined tensile strength values quantitatively in terms of these components.

Consider first the *inherently cohesive materials.* Rumpf (10) proposed a basic equation for calculating the tensile strength of a bed of ideal monosize spheres:

$$T = \frac{9}{8}\left(\frac{1-\epsilon}{\pi d^2}\right)KH \qquad \text{(Eq. 1)}$$

where T = tensile strength, ϵ = porosity, d = sphere diameter, K = coordination number, and H = mean bonding force at point of contact. The value of H is dependent on the nature of interparticle attraction, and it is necessary to analyze the main interparticle effects separately.

van der Waals' Forces—When the mean bonding force H is due to van der Waals' forces, its value (11) becomes:

$$H = \frac{Ad}{24g^2} \qquad \text{(Eq. 2)}$$

where A is a constant about 10^{-12} dyne cm., and g is the distance

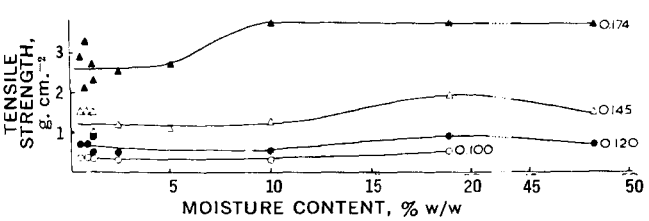

Figure 5—*Effect of moisture content (% w/w, dry basis) on tensile strength of calcium phosphate at the packing densities shown.*

Table II—Surface Tensions and Viscosities of the Water and Saturated Salt Solutions Used

Fluid Used for Wetting	Surface Tension, dynes cm.$^{-1}$ 1	2	3	Mean	Temperature	Absolute Viscosity, cps., over Rates of Shear, 0–900 sec.$^{-1}$ (All Newtonian)
Distilled water	71.2	70.8	71.0	71.0	23.0°	0.95 at 27.5°
Saturated potassium chloride solution	77.0	77.2	76.9	77.0	27.0°	1.00 at 28°
Saturated sodium chloride solution	80.1	80.2	80.2	80.2	27.5°	1.87 at 27.5°

between the sphere surfaces and is less than 1000 Å.

By substituting this value of H into Rumpf's basic equation (1):

$$T = \frac{9}{8}\left(\frac{1-\epsilon}{\pi d^2}\right)\frac{KAd}{24g^2} \qquad \text{(Eq. 3)}$$

To a first approximation, Rumpf (10) considered that:

$$K\epsilon = \pi \qquad \text{(Eq. 4)}$$

Thus, by combining Eqs. 3 and 4:

$$T = \frac{9}{8}\left(\frac{1-\epsilon}{\epsilon}\right)\frac{A}{24g^2d} \qquad \text{(Eq. 5)}$$

Because there was no way to measure the value of the term g for the materials used in this study, the contribution that the van der Waals' forces would make to tensile strength could not be assessed directly. Furthermore, the bulk solids used were not ideal monosize spheres. However, by considering an ideal system which possesses the same tensile strength as the real system and which consists of spheres with the same diameter as the mean particle diameter of the real system, it is possible to obtain, from Eq. 5, values for g which may be termed the mean equivalent separation distance.

On rearrangement, Eq. 5 becomes:

$$g = \sqrt{\frac{9A(1-\epsilon)}{192d\epsilon T}} \qquad \text{(Eq. 6)}$$

Tensile strength values may only be substituted into this equation when it is realistic to suppose that the attractive forces arise *solely* from van der Waals' forces, *i.e.*, for the cohesive materials when *dry*.

Table III—Mean Equivalent Separation Distances Calculated from Eq. 6 for Inherently Cohesive Materials When Dry

Material	Packing Density, ρ_B/ρ_P	Porosity, $\epsilon = 1 - \rho_B/\rho_P$	Observed Tensile Strength, T, g. cm.$^{-2}$	Mean Equivalent Separation Distance Calculated from Eq. 5, g, cm.
Sodium chloride (end-runner milled batch 1), $d = 1.4 \times 10^{-3}$ cm.[a]	0.229	0.771	2.0	7.1×10^{-8}
	0.251	0.749	3.2	6.0×10^{-8}
	0.275	0.725	4.8	5.2×10^{-8}
	0.302	0.698	7.3	4.5×10^{-8}
	0.331	0.669	11.3	3.9×10^{-8}
Sodium chloride (micronized), $d = 5 \times 10^{-4}$ cm.[a]	0.131	0.869	1.9	8.7×10^{-8}
	0.159	0.841	3.5	7.2×10^{-8}
	0.209	0.791	8.7	5.4×10^{-8}
Potassium chloride (end-runner milled), $d = 1.5 \times 10^{-3}$ cm. (Fig. 4)	0.209	0.791	1.0	9.2×10^{-8}
	0.251	0.749	2.2	7.0×10^{-8}
	0.275	0.725	3.3	6.1×10^{-8}
	0.331	0.669	7.8	4.5×10^{-8}
	0.398	0.602	18.4	3.4×10^{-8}

[a] Results taken from Eaves and Jones (1).

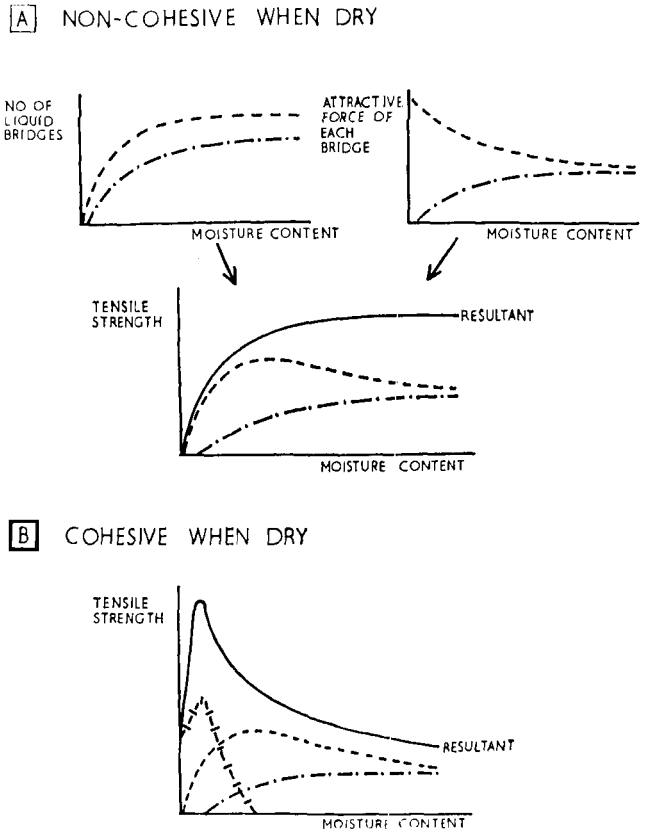

Figure 6—*Diagrammatic representation of the suggested contributions of various particle-particle interactions to tensile strengths of beds of bulk solids. Key: A, bulk solid which is noncohesive when dry; B, bulk solid which is cohesive when dry; - - -, liquid bridges at points of actual contact; -·-, liquid bridges at points of near contact; and -|-|, particle-particle interactions due to van der Waals' bonding and mechanical interactions.*

A selection of typical results are shown in Table III, from which it can be seen that the mean equivalent separation values vary from 3 to 10 Å. These separation distances are of the order of magnitude of the distance over which molecular forces might be expected to act. It appears, therefore, that to a first approximation the experimental results for the dry cohesive materials fit Eq. 5 reasonably well.

Pendular Bonds—When the mean bonding force H is due to pendular bonds, its value (12) is:

$$H = \alpha d f\left(\delta, \theta, \frac{g}{d}\right) \qquad \text{(Eq. 7)}$$

where α = the surface tension of the liquid, d = the sphere diameter, δ = the contact angle, θ = the half centriangle (*i.e.*, half the angle subtended at the sphere center by the liquid bridge), and g = the distance between the sphere surfaces.

By substituting this value of H into Rumpf's basic equation (Eq. 1):

$$T = \frac{9}{8}\left(\frac{1-\epsilon}{\pi d}\right)K\alpha f\left(\delta, \theta, \frac{g}{d}\right) \qquad \text{(Eq. 8)}$$

From Eq. 4, $K\epsilon = \pi$; thus:

$$T = \frac{9}{8}\left(\frac{1-\epsilon}{\epsilon}\right)f\left(\delta, \theta, \frac{g}{d}\right) \qquad \text{(Eq. 9)}$$

Pietsch and Rumpf (12) calculated values of the function $f(\delta, \theta, g/d)$ for various porosities and liquid contents using the model of monosize spheres, assuming that $\delta = 0$. Typical results (13) are

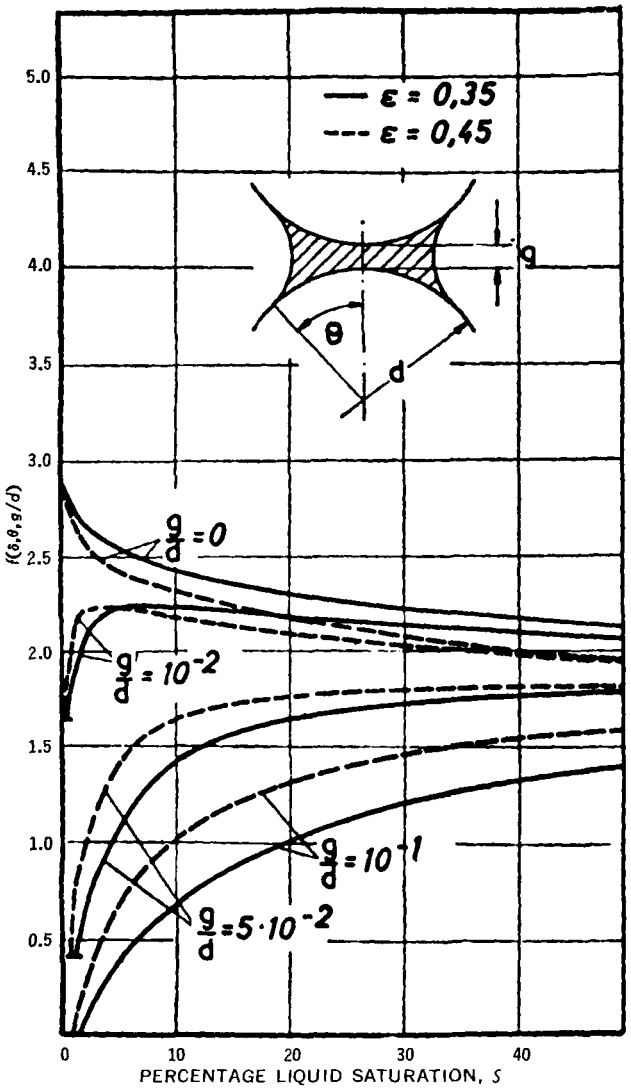

Figure 7—*Values of the function* f(δ, θ, g/d) *at various liquid contents for a bed of uniform spheres at two different porosities* (ε). *Reproduced with modified notation from Pietsch (13).*

shown in Fig. 7, in which the liquid content is expressed as the percentage liquid saturation, *s; i.e.*,

$$\frac{\text{pore volume occupied by the liquid}}{\text{total pore volume}}$$

The relationship between percentage liquid saturation, *s*, and liquid content, *b* (% w/w dry basis), is (14):

$$s = 100 \frac{\rho_P}{\rho_L} \cdot \frac{1 - \epsilon}{\epsilon} \cdot b \qquad \text{(Eq. 10)}$$

where ρ_P = particle density, ρ_L = density of liquid, and ϵ = porosity.

Thus, for the cohesive materials, if it is assumed that at a fixed packing density the mean equivalent particle separation distance, *g*, is the same for dry beds as for moist beds (*i.e.*, *g* has the same numerical value in Eqs. 5 and 9), it is possible to estimate the tensile strength due to pendular bonds, as shown in the following example: potassium chloride, end-runner milled (mass median diameter 15 μ) at a packing density of 0.398.

At a moisture content of 12.0%, the curve showing the relationship between tensile strength and moisture content at a fixed packing density (Fig. 4) has begun to level out following the decrease due to disruption of van der Waals' forces (see also Fig. 6). Thus, the tensile strength is probably due to pendular bonds only.

From Table III, the mean equivalent particle separation based on

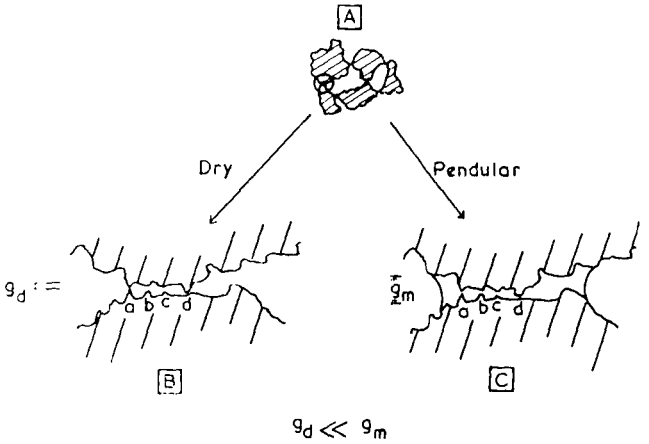

Figure 8—*Diagrammatic representation of the conditions at points of contact at dryness* (*B*) *and in the presence of liquid bridges* (*C*).

a consideration of the van der Waals forces is 3.4×10^{-8} cm. Since $d = 1.5 \times 10^{-3}$ cm.:

$$\frac{g}{d} = \frac{3.4 \times 10^{-8}}{1.5 \times 10^{-3}} = 2.3 \times 10^{-5} \qquad \text{(Eq. 11)}$$

Now 12% w/w moisture content ≡ 15.5% liquid saturation. From Fig. 7, therefore, $f(\delta, \theta, g/d)$ lies between 2.2. and 2.4. From Eq. 9:

$$T = \frac{9}{8}\left(\frac{1 - \epsilon}{\epsilon}\right)\frac{\alpha}{d} f\left(\delta, \theta, \frac{g}{d}\right) \qquad \text{(Eq. 12}a\text{)}$$

$$T = 38.9 f\left(\delta, \theta, \frac{g}{d}\right) \qquad \text{(Eq. 12}b\text{)}$$

Thus, *T* should lie between 85.6 and 93.4 g. cm.$^{-2}$. From Fig. 4, however, the experimentally determined value of *T* is 16.0 g. cm.$^{-2}$. Therefore, the assumption that the mean equivalent particle separation distance, *g*, was the same at a fixed porosity whether the tensile strength was calculated using the Hamaker concept for the dry system (*i.e.*, Eq. 5) or the Pietsch and Rumpf (12) concept for the pendular system (*i.e.*, Eq. 9) is invalid.

In a similar way, it may be shown that the tensile strengths of the fine sodium chloride (both end-runner milled and micronized) calculated in this manner are also overestimated.

If the experimentally determined values of tensile strength of the inherently cohesive materials at moisture contents above 10% w/w (dry basis) are substituted into Eq. 9, values of $f(\delta, \theta, g/d)$ may be obtained. Then, by reference to Fig. 7, the ratios *g*/*d* and, hence, *g* may be obtained (Table IV). By comparing these results with those

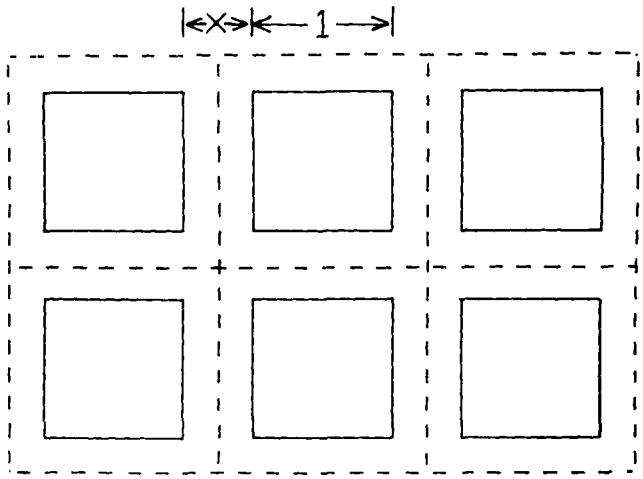

Figure 9—*Idealized system of monosize cubes used for the calculation of theoretical interparticle distances.*

Table IV.—Mean Equivalent Separation Distances Obtained from Fig. 7, after Calculation of the Function $f(\delta, \theta, g/d)$ from Eq. 9 for Inherently Cohesive Materials at Moisture Contents of 10% w/w Dry Basis and Above

Material	Packing Density, ρ_B/ρ_T	Porosity, $\epsilon = 1 - \rho_B/\rho_P$	Observed Tensile Strength, T, g. cm.$^{-2}$	$f(\delta, \theta, g/d)$ Calculated from Eq. 9	Percentage Liquid Saturation Calculated from Eq. 10	Approximate Ratio, g/d, from Fig. 7	Approximate Mean Equivalent Separation Distance, g, μ
Sodium chloride (end-runner milled), $d = 1.4 \times 10^{-3}$ cm., moisture content = 10% w/w (dry basis)[a]	0.331	0.669	7.8	0.24	10.6	$>10^{-1}$	>1.4
Sodium chloride (micronized), $d = 5 \times 10^{-4}$ cm., moisture content = 10% w/w (dry basis)[a]	0.331	0.669	6.0	0.07	10.6	$>10^{-1}$	>0.5
Potassium chloride (end-runner milled), $d = 1.5 \times 10^{-3}$ cm., moisture content = 12% w/w (dry basis) (Fig. 4)	0.398	0.602	16.4	0.42	15.5	$>10^{-1}$	>1.5

[a] Results taken from Eaves and Jones (1).

for the same materials at the same packing density when *dry* (Table III), it may be seen that the mean equivalent separation distance is about 1000 times greater for the *moist* systems. However, for a given bulk solid at a fixed packing density, the absolute mean particle separation distance cannot change and must be independent of the moisture content. This apparent discrepancy arises because the values obtained for g using first the Hamaker concept for van der Waals' attraction (Eq. 5) and then the approach by Rumpf and Pietsch (12) based on a consideration of pendular bonds (Eq. 9) are not measures of the same parameter. This is illustrated more clearly in Fig. 8.

Consider an assembly of real dry irregular particles, A, at a fixed packing density. The conditions at each point of contact will be similar and will change in the presence of moisture. In the perfectly dry state, the value of g determined by means of Eq. 5 is the mean equivalent value for a system of ideal spheres and is based on the average separation distance for every microcontact (*e.g.*, a, b, c, and d in Fig. 8B) at which van der Waals' attraction exists. In the pendular state, however, the value obtained for g from Eq. 9 is the equivalent value based on the average lengths of the macroscopic liquid bridges (Fig. 8C) which swamp all the microcontacts a, b, c, and d. The mean separation distance for the real system may thus be very different in the dry and moist states; *i.e.*, $g_d \ll g_m$. This explains, therefore, why the tensile strength of materials possessing moisture as pendular bonds, obtained by substitution of the value obtained for g from Eq. 5 into Eq. 9, was grossly overestimated.

The *inherently noncohesive materials* are simpler because the contribution due to van der Waals' forces is insignificant. Typical mean equivalent particle separation distances calculated from Eq. 9 are compared in Table V, with the theoretical interparticle distances obtained from the following geometrical considerations.

Assume that: (*a*) the particles are monosize cubes with the cube side length, l, equal to the mass median diameter of the real particles, and (*b*) the particles form an ideal uniform cubic packing. Then the assembly may be considered to consist of many unit cells, each possessing a particle at its center (Fig. 9).

For each unit cell, using the symbols shown:

$$\text{packing density, } \rho_B/\rho_P = \frac{\text{volume of cubic particle}}{\text{volume of unit cell}} = \frac{l^3}{(l + x)^3} \qquad \text{(Eq. 13)}$$

Thus:

$$(l + x)^3 = \frac{l^3}{\rho_B/\rho_P} \qquad \text{(Eq. 14)}$$

Hence, interparticle distance:

$$x = \left(\sqrt[3]{\frac{l^3}{\rho_B/\rho_P}}\right) - l \qquad \text{(Eq. 15)}$$

By bearing in mind that the values of g in Table V are only approximate and taking into account the assumptions made in the calculation of x, it can be seen that the mean equivalent separation distances, g, obtained from Eq. 9 are realistic in terms of the interparticle separation distances, x, calculated from the geometry of the packings. Furthermore, the values of x calculated from the ideal

Table V.—Mean Equivalent Separation Distances Obtained from Fig. 7 after Calculation of the Function $f(\delta, \theta, g/d)$ and Theoretical Interparticle Distances for the Inherently Noncohesive Sodium Chloride Fractions[a]

Size Fraction, μ	Mean Size, d, cm.	Moisture Content (% w/w), Dry Basis	Packing Density, ρ_B/ρ_P	Porosity, $\epsilon = 1 - \rho_B/\rho_P$	Observed Tensile Strength, T, g. cm.$^{-2}$	Function $f(\delta, \theta, g/d)$ Calculated from Eq. 9	Percentage Liquid Saturation Calculated from Eq. 10	Approximate Ratio, g/d, from Fig. 7	Approximate Mean Equivalent Separation Distance, g, μ	Theoretical Interparticle Distance, x, μ
32–75	5.35×10^{-3}	10.0	0.457	0.543	17.0	1.2	18.1%	$>10^{-1}$	>5	16
75–178	1.27×10^{-2}	10.0	0.457	0.543	5.6	0.9	18.1%	$>10^{-1}$	>13	38
178–250	2.14×10^{-2}	10.0	0.457	0.543	4.5	1.2	18.1%	$>10^{-1}$	>21	64
250–353	3.02×10^{-2}	10.0	0.457	0.543	3.5	1.4	18.1%	$>10^{-1}$	>30	90
75–178	1.27×10^{-2}	2.0	0.501	0.499	5.4	0.7	4.7%	10^{-1}	13	33
75–178	1.27×10^{-2}	2.0	0.479	0.521	4.5	0.7	4.3%	10^{-1}	13	35
75–178	1.27×10^{-2}	2.0	0.437	0.563	3.3	0.6	3.7%	10^{-1}	13	40
75–178	1.27×10^{-2}	2.0	0.380	0.620	1.9	0.4	2.9%	10^{-1}	13	47

[a] Results taken from Eaves and Jones (1).

cubically packed system represent the maximum possible values that can be achieved with a model of monosize cubes.

It appears, therefore, that Eq. 9 will satisfactorily estimate the tensile strengths of the moist, inherently noncohesive sodium chloride fractions.

CONCLUSION

Two nonporous bulk solids of similar particle size but different coherences were shown to exhibit, at similar porosities, different changes in tensile strength with increasing moisture content. The more cohesive material (potassium chloride) showed similar changes to the fine sodium chloride fractions studied previously (1), whereas the less cohesive one (glass) resembled the coarse sodium chloride fractions.

Mechanisms for the tensile strength changes are suggested, and the type of change obtained appears to be dependent on the magnitude of the inherent coherence of the dry material and not necessarily on its particle size.

The cohesive calcium phosphate differed from the other cohesive bulk solids studied, however, in that its tensile strength at a fixed porosity was independent of the moisture content over a wide range. This finding was attributed either to the porous nature of the particles preventing location of the moisture at the particle surface or to a fortuitous balance between the components of tensile strength which increase with moisture content and those that decrease.

REFERENCES

(1) T. Eaves and T. M. Jones, *J. Pharm. Sci.*, **61**, 256(1972).

(2) T. Eaves and T. M. Jones, *J. Pharm. Pharmacol.*, **22**, 594 (1970).

(3) T. Eaves and T. M. Jones, *Rheol. Acta*, **10**, 127(1971).

(4) R. Farley and F. H. H. Valentin, *Powder Technol.*, **1**, 344 (1967/68).

(5) D. M. Newitt and J. M. Conway-Jones, *Trans. Inst. Chem. Eng.*, **36**, 422(1958).

(6) E. Bock, *Adhesion*, **7**, 289(1965).

(7) R. Aoki and H. Tsunakawa, *J. Soc. Mater. Sci. Japan*, **18**, 497(1969).

(8) J. Craik and B. F. Miller, *J. Pharm. Pharmacol.*, **10**, 136T (1958).

(9) V. E. Glushkov, N. I. Karnaushenko, and P. V. Platonov, Paper B.4.3., 3rd Congress CHISA, Marianbad, Czechoslovakia, Sept. 1969.

(10) H. Rumpf, in "Agglomeration," W. A. Knepper, Ed., Interscience, London, England, 1962.

(11) H. C. Hamaker, *Physica*, **4**, 1027(1937).

(12) W. B. Pietsch and H. Rumpf, *Chem.-Ing.-Tech. Z.*, **39**, 885 (1967).

(13) W. B. Pietsch, *Staub*, **27**, 24(1967).

(14) W. B. Pietsch, E. Hoffmann, and H. Rumpf, *Ind. Eng. Chem. Prod. Res. Develop.*, **8**, 58(1969).

ACKNOWLEDGMENTS AND ADDRESSES

Received July 15, 1971, from the *Department of Pharmacy, University of Nottingham, Nottingham NG7 2RD, England.*

Accepted for publication October 19, 1971.

The authors thank The Boots Co. Ltd. for the tensile testing apparatus and the Agnes Borrowman Trust for a grant to T. Eaves.

* Present address: Sandoz Products Ltd., Horsforth, Leeds, England.

▲ To whom inquiries should be directed.

Effect of Lysergide and Nimergoline on Glucose Metabolism Investigated on the Dog Brain Isolated *In Situ*

G. BENZI▲, M. De BERNARDI, L. MANZO, A. FERRARA, P. PANCERI, E. ARRIGONI, and F. BERTÉ

Abstract □ The glucose uptake and lactic and pyruvic acid formation were investigated in the dog brain isolated *in situ* during: (*a*) control conditions, (*b*) hypoxia by suppression of blood oxygenation, and (*c*) recovery of oxygenation and intracarotid treatment with saline solution or lysergide (5×10^{-7} *M*) or nimergoline (5×10^{-5} *M*) at the rate of 0.5 ml./min. for 30 min. The hypoxia induced at first an increase and subsequently a decrease in brain glucose uptake, with an increase in both lactic and pyruvic acid formation. The subsequent *recovery of blood oxygenation*, with intracarotid perfusion with saline solution, induced only a partial recovery of glucose metabolism supported by the increase of the depressed glucose uptake and the decrease of the enhanced lactic and pyruvic acid formation. No significant difference could be demonstrated *versus* the intracarotid perfusion with lysergide. The intracarotid perfusion with nimergoline induced both an increase in cerebral glucose uptake and a decrease in pyruvate formation, with statistical difference with respect to the change induced by saline solution perfusion; the lactic acid formation remained in the same order of magnitude induced by saline solution perfusion.

Keyphrases □ Glucose metabolism, isolated dog brain *in situ*—effect of lysergide and nimergoline □ Lysergide—effect on glucose metabolism in isolated dog brain *in situ* □ Nimergoline—effect on glucose metabolism in isolated dog brain *in situ* □ Lactic acid formation, isolated dog brain *in situ*—effect of lysergide and nimergoline □ Pyruvic acid formation, isolated dog brain *in situ*—effect of lysergide and nimergoline

The predominant source of energy for the brain comes from carbohydrate metabolism, the glucose being the major, if not exclusive, energy-yielding substance removed from the blood to the brain. In fact, according to Kety (1), the respiratory quotient of the brain is near one. On the other hand, according to Bloom (2) and Sacks (3), brain slices appear to catabolize glucose practically up to the end *via* the Embden–Meyerhof